Model of the ARF-Aux/IAA signaling network

Abstract

This note deals with more technical aspects of the ordinary differential equations (ode) presented in the main text as a model of auxin signaling. A more detailed account of the relation between auxin levels and Aux/IAA decay rates is derived. A proof of uniqueness of the steady state in a region of state space containing all performed simulations is provided. Finally, numerical simulations are used to investigate the influence of the different parameters on the model, when they vary in plausible ranges.

1 Model properties

We refer the reader to the main text for a description of the model, and its parameters. A visual representation of the elementary reactions considered in this model is shown in Figure 1. We also recall the equations, since specific references to some of them will be needed in this note:

$$\frac{dI}{dt} = \pi_I R + 2k'_{II}D_{II} - 2k_{II}I^2 + k'_{IA}D_{IA} - k_{IA}IA + \delta_{II}(x)D_{II} - \delta_I(x)I \quad (1)$$

$$\frac{dA}{dt} = \pi_A + k'_{IA}D_{IA} - k_{IA}IA + \delta_{IA}(x)D_{IA} - \delta_A A \quad (2)$$

$$\frac{dD_{II}}{dt} = k_{II}I^2 - (k'_{II} + \delta^*_{II} + \delta_{II}(x))D_{II} \quad (3)$$

$$\frac{dD_{IA}}{dt} = k_{IA}IA - (k'_{IA} + \delta^*_{IA} + \delta_{IA}(x))D_{IA} \quad (4)$$

$$\frac{dR}{dt} = h(I, A, D_{IA}) - \delta_R R \quad (5)$$

where h is the transcription rate of the target genes, and takes the form:

$$h(I, A, D_{IA}) = \frac{1 + \frac{f}{B_d}A\left(1 + \frac{\omega_A f_A}{B_d}A\right)}{1 + \frac{A}{B_d}\left(1 + \frac{\omega_A}{B_d}A\right) + \frac{\omega_I}{K_d B_d}AI + \frac{\omega_D}{B_d}D_{IA} + \kappa_A^-}. \quad (6)$$

1.1 Auxin dependent decay rates

Recall that Aux/IAA decay rates depend on the level of auxin x as follows:

$$\delta_I(x) = \gamma_I \delta_I \frac{Kx}{1 + Kx}, \quad (7)$$

and similarly for D_{IA} and D_{II} dimers. The form above has been obtained by a quasi-steady state analysis of the full pathway leading to Aux/IAA proteolysis. The underlying assumption is that binding events occur faster than subsequent ubiquitination and degradation. More precisely, recall that the action of auxin on this network is mediated by the TIR1/AFB receptor,

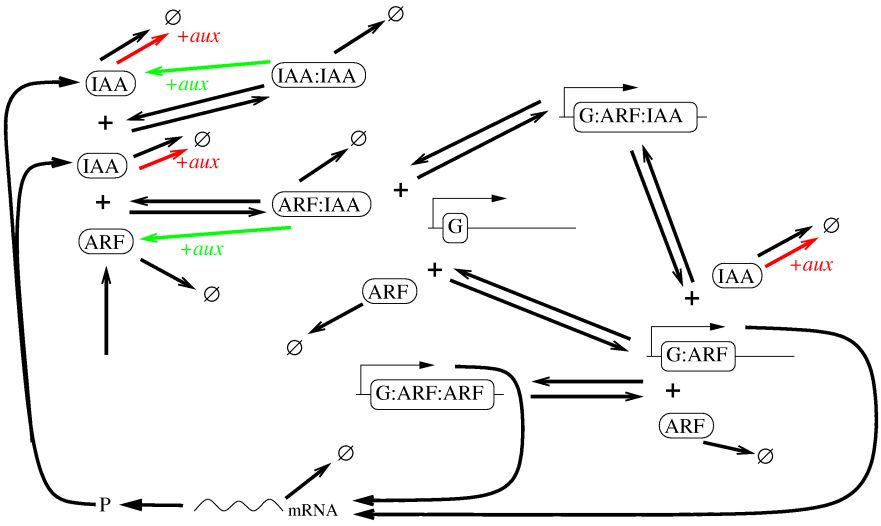

Figure 1: The reaction scheme considered for the auxin signaling pathway. ARF and Aux/IAA (IAA above) can form dimers in a reversible way. A pool of auxin responsive genes is denoted by G, to which ARF bearing complexes can bind, via two pathways for ARF:IAA. Arrows represent the possible transformations between elements, and + represent binding of proteins and/or promoter of the G pool of genes. Degradation is represented by $\to \varnothing$. Colored arrows indicate the effect of auxin on the system: Aux/IAA proteins are degraded when they are monomers or their partner is freed when they are bound in a dimer.

on which auxin acts as a 'glue' between Aux/IAA and the $\mathrm{SCF}^{\mathrm{TIR1/AFB}}$ complex, leading to their ubiquitination, rapidly followed by proteasome mediated degradation. Let us call these events the *perception module*. To analyse this module, we used a scheme in which the main elementary reactions involved in auxin perception are considered. Let us use abbreviations and denote auxin by x, TIR1/AFB by T and Aux/IAA by I. Also, let $\widetilde{I}$ denote ubiquitinated Aux/IAA. Then, auxin perception is described by the reactions below:

$$\begin{array}{ccccc} x+T & \underset{k_d}{\overset{k_a}{\rightleftharpoons}} & x{:}T & & \\ x{:}T+I & \underset{\ell_d}{\overset{\ell_a}{\rightleftharpoons}} & x{:}T{:}I & \overset{\ell_m}{\to} & x{:}T+\widetilde{I} \\ I & \overset{\delta_I}{\to} & \varnothing & & \\ \widetilde{I} & \overset{\delta_{\widetilde{I}}}{\to} & \varnothing & & \end{array}$$

Then, assuming that both $x:T$ and $x:T:I$ complexes form rapidly, and are essentially at equilibrium, one obtains kinetic rates similar to the Michaelis-Menten law. Indeed, using mass action law,

$$\frac{d[x:T]}{dt} \approx 0 \quad \text{and} \quad \frac{d[x:T:I]}{dt} \approx 0$$

leads to

$$[x:T] \approx \frac{k_a}{k_d}[x][T] \quad \text{and} \quad [x:T:I] \approx \frac{\ell_a}{\ell_d+\ell_m}[x:T][I]$$

Then, denoting $K = \frac{k_a}{k_d}$, $L = \frac{\ell_a}{\ell_d+\ell_m}$ and the total TIR1/AFB concentration, $T_{tot} = [T] + [x:T] + [x:T:I]$, which we suppose is constant, we get

$$[x:T:I] = KL[x][T][I] \quad \text{and} \quad T_{tot} = [T]\left(1 + K[x] + KL[x][I]\right),$$

leading to

$$[x:T:I] = \frac{T_{tot}KL[x][I]}{1+K[x]+KL[x][I]}.$$

From these relations and the reaction scheme, the following equations are deduced:

$$\begin{aligned} \frac{dI}{dt} &= -\frac{\ell_m T_{tot} KL\, xI}{1+Kx+KL\, xI} - \delta_I I \\ \frac{d\widetilde{I}}{dt} &= \frac{\ell_m T_{tot} KL\, xI}{1+Kx+KL\, xI} - \widetilde{\delta}_I \widetilde{I} \end{aligned} \tag{8}$$

where the brackets have been dropped for simplicity.
Since ubiquitination leads to rapid proteasome mediated degradation, it is rather natural to consider that $\widetilde{\delta_I} \gg \delta_I$, or in other terms that δ_I is low and the apparent decay rate of Aux/IAA is well approximated by

$$\frac{\ell_m T_{tot} KL\, x}{1+Kx+KL\, xI}.$$

This decay depends on I, but a first order approximation at $I \approx 0$, which is the equilibrium of equation (8), leads us the the following rate:

$$\delta_I(x) = \ell_m T_{tot} L \frac{Kx}{1+Kx},$$

which we have rewritten in more intuitive terms under the form shown in (7). Note that setting x to 0 would lead to $\delta_I(x) = 0$, whereas we have chosen a reference decay rate $\delta_I > 0$. Hence, the minimal level of auxin in our simulations, x_{basal}, was set to ensure that $\delta_I(x_{basal}) = \delta_I$, i.e. $x_{basal} = 1/(K(\gamma_I - 1))$.

Observe that the parameters x and K play perfectly symmetric roles. Hence the value x, though representing auxin levels, could as well be interpreted in terms of the affinity of auxin to its TIR1/AFB co-receptors.

The preceding analysis has led us to use the function above to describe auxin dependent decay rates. This relies on our assumption that auxin binding to TIR1, and subsequent recruitment of Aux/IAA for ubiquitination are faster than ubiquitination and degradation of Aux/IAA. Moreover, under this assumption our model provides essentially the same dynamics of the perception module as a previously published model, which considers the same reaction scheme for this module, without quasi steady state reduction [3].

1.2 Existence of a unique steady state

We present here a qualitative analysis of the model, which shows that equations (1)-(5) admit a unique equilibrium for a large set of parameter values, as proved below. Then, the effect of auxin may only be to perturb this equilibrium. This perturbation may be quantitative, changing the levels of the different substances at equilibrium, or it could be qualitative, changing the stability properties of the equilibrium. If the latter is unstable, sustained oscillations may be observed in the system, and the parameter values at which this occurs correspond to a Hopf bifurcation. Although such bifurcations were not observed in our simulations, they cannot be excluded in principle – for parameter values we have not tested.

Let us now sketch a proof of the existence and uniqueness of the equilibrium point.

Proof. The basic idea of the proof is to perform direct computations of the equilibrium equations, which lead to all variables being expressed in terms of I and R only, themselves solution

of a system of the form $\{R = f(I),\ R = g(I)\}$. Then we show that f is always increasing, and for a large set of parameters (including all the plausible ones used in simulations), g is decreasing, which ensures the existence and uniqueness of an equilibrium solution.

Let us now try to directly solve the equilibrium equations associated to (1)-(5), i.e. when the left-hand side is zero. First solving equations (3) and (4) gives:

$$D_{II} = \frac{k_{II} I^2}{k'_{II} + \delta^*_{II} + \delta_{II}(x)} \qquad \text{and} \qquad D_{IA} = \frac{k_{IA} IA}{k'_{IA} + \delta^*_{IA} + \delta_{IA}(x)}$$

From which we deduce

$$k'_{IX} D_{IX} - k_{IX} IX + \delta_{IX}(x) D_{IX} = -\frac{k_{IX}\delta^*_{IX}}{k'_{IX} + \delta^*_{IX} + \delta_{IX}(x)} IX$$

for both $X = I$ and $X = A$. Then, using the abbreviation $\alpha_{IX} = \frac{k_{IX}\delta^*_{IX}}{k'_{IX}+\delta^*_{IX}+\delta_{IX}(x)}$ and considering equations (1) and (2), one gets:

$$-\pi_I R + \alpha_{II} I^2 + \alpha_{IA} IA + \delta_I(x) I = 0 \qquad \text{and} \qquad -\pi_A + \alpha_{IA} IA + \delta_A A = 0$$

From the second equation, $A = \frac{\pi_A}{\delta_A + \alpha_{IA} I}$ follows and can be injected in the first equation, to lead to:

$$\alpha_{IA}\alpha_{II} I^3 + (\alpha_{II}\delta_A + \alpha_{IA}\delta_I(x)) I^2 + (\delta_A \delta_I(x) + \pi_A \alpha_{IA}) I - (\delta_A + \alpha_{IA} I)\pi_I R = 0$$

Hence, at this point D_{II} and D_{IA} can be deduced from I, A and R, and A is uniquely determined by I. Thus, the problem is reduced to a system of two equations in I and R: the one above and that corresponding to (5). From the equation above, we can deduce that R is an increasing function of I, as a sum of three functions increasing with I. On the other hand, from equation (5) and the expressions above we get after some further calculations

$$h(I, A, D_{IA}) = h\left(I, \frac{\pi_A}{\delta_A + \alpha_{IA} I}, \frac{\pi_A \alpha_{IA} I}{\delta^*_{IA}(\delta_A + \alpha_{IA} I)}\right) \tag{9}$$

We will show below that the function above is a decreasing function of I for a large set of parameters, including all those we have used in numerical simulations. Since at equilibrium $R = \frac{1}{\delta_R} h(I, A, D_{IA})$, it follows that for the mentioned parameters, at steady-state R is defined as the intersection of two positive functions of I, one increasing and the other decreasing. Thus, there exists one solution to the steady state equations, and it is unique.

Proof that h decreases with I in (9):
By computing the partial derivatives of $h(I, A, D_{IA})$, it is possible to see that it decreases with both I and D_{IA}, but is not monotonous in A in general. Namely, h increases with A whenever

$$A > \frac{B_d}{\sqrt{\omega_A f_A f}}, \tag{10}$$

and when the converse inequality holds, it decreases with A if and only if the following inequality holds:

$$\pi_A \leqslant \delta_A A + \left(\frac{f-1}{\frac{\omega_I}{K_d} + \frac{\omega_D \alpha_{IA}}{\delta^*_{IA}}}\right) \frac{\frac{2\omega_A f_A}{B_d}\alpha_{IA} A^2 + \alpha_{IA} A}{1 - \frac{\omega_A f_A f}{B_d^2} A^2} \tag{11}$$

It is possible to show that the right-hand side above increases with A, by computing its derivative with respect to A. Moreover, it equals 0 when $A = 0$, and tends to infinity as $A \to \frac{B_d}{\sqrt{\omega_A f_A f}}$ by lower values. Thus by the intermediate value theorem, there must be a unique $A^* \in [0, \frac{B_d}{\sqrt{\omega_A f_A f}}]$

at which it equals $\pi_A > 0$, and for all $A \geqslant A^*$ the inequality (11) is satisfied.
However, A^* is a root of a degree three polynomial, and there is no simple expression for this value. Hence, to have a better intuition, we may use instead the coarser inequality (10), in particular to evaluate the range of parameter values for which h increases with A, see below.
Finally, since in (9) the three arguments are respectively increasing, decreasing and increasing functions of I, while h respectively decreases, increases and decreases with respect to the same arguments under constraint (11), we conclude that it is *in fine* decreasing with I under this constraint, or the coarser constraint (10). □

As we will see in the next section, a typical value for the bounding value in (10) is $\frac{100}{\sqrt{1000}} \approx 3.2$. In our simulations, the ARF concentrations were typically much larger than this value (of the order of 100). Moreover, the condition being sufficient, but not necessary, the uniqueness of the steady-state remains true even for some parameters violating (10), and may in fact hold for all parameters, although our proof cannot ensure this.

2 Influence of the different parameters

The behaviour of the model depends on all the parameters described in Section 1, and a full exploration of the parameter space is clearly impossible. However, a number of quantitative indications can be found in the literature, which have allowed us to restrict the ranges of parameter values to small but plausible sets. Namely, measurements have been performed of the half-life[1] of various Aux/IAA proteins with and without auxin [2], indicating that these half-lives vary between less than 15 minutes and more than 20h, although most of them being shorter than 1h. These parameters were approximately doubled upon auxin induction, however since a fixed dose of this hormone was added to the system, we can only deduce from this that γ_I is at least two in equation (7). Also ARF1 half-life has been measured [5] and is of 3-4h, which we hypothesized to be an indicative value for all ARF proteins, in absence of any other data of this type. Also, [4] provides mRNA half-life of essentially all genes of *Arabidopsis thaliana*, from which we extracted the values of the Aux/IAA coding genes. Their average half-life was of $\approx$ 4h30, which we took as a reference to fix the δ_R value.
The remaining parameters are production rates and protein-protein association constants, as well as the coefficients appearing in the function h. In absence of *Arabidopsis thaliana* specific values for such parameters, we used values in the ranges typically found in the literature, even though these values sometimes concern other biological systems, such as yeasts or animals. It is usual that these values vary by several orders of magnitude, and thus we have investigated the effects of such variations on the system.

Hence, all decay rates were fixed according to the experimental figures available in the literature, except δ_I, for which we tried different values in the range mentioned above. We also varied the other parameters, and studied how the behaviour of the network was affected by these variations. To do so, we fixed all the parameters to a reference value, and changed them one by one. The set of reference parameters we used is recapitulated in the table below:

k_{IX}	K_{IX}	δ_I	δ_A	δ_R	δ^*_{IX}	π_I
1	10	0.05	0.003	0.007	0.003	1

π_A	f, f_A	$\omega_A, \omega_D, \omega_I$	γ_I	K	B_d	κ_A^-
1	10	10	10	1	100	10

(12)

Where $X \in \{I, A\}$, and $K_{IX} = \frac{k'_{IX}}{k_{IX}}$ is the dissociation constant of the dimer D_{IX}. The decay rates were converted, so that the time units are minutes, and the concentration units are nM.

[1] The half life τ_X of a molecule X is related to its decay rate δ_X by the relation $\delta_X = \frac{\ln 2}{\tau_X}$.

Note however that since expression data was essentially qualitative, this choice of units aims at using a coherent set of parameters, but the precise absolute concentration values we obtain in the simulations should not be considered as accurately reflecting the real figures.
The fact that the dimer decay rates were rather low was suggested by [1], in which it is demonstrated that dimers may in general present a higher level of stability than the monomers they are mode of. However, numerical simulations using higher decay rates did not induce significant differences in the dynamics in our case, see below.
The basal auxin level is $x_{basal} \approx 0.11$ with the parameters above.

In order to give an idea of the influence of the different parameters, we considered different values around the reference figure in (12). For each parameter, we typically consider the influence of a step-like increase of auxin on the system for various values of the parameter, to observe its influence on the response of the network.
We also consider the effect of auxin level fluctuations, in order to evaluate the robustness properties of the system. Several input functions were tested, whose precise shape did not have a significant impact on the buffering properties of the network. Hence we use a sinusoid function in this note, for simplicity. In these cases, the range over which auxin fluctuates was chosen so that the auxin-dependent decay rates $\delta_I(x)$ were varying between their basal and maximal values.

For all the simulations reported here, we use the colormap shown in Figure 2.

Figure 2: All simulations are represented using this color map, where the maximal and minimal value depend on the variable or parameter whose level is represented by a color.

Basal ARF activators level π_A

As mentioned in the main text, this parameter has a drastic effect on the response of the system to auxin changes. In short, low values of this parameter lead the system to be to a large extent auxin-insensitive, and at higher values, it directly relates to the level of "response" of the system to auxin increase. This is interesting, since in our *in situ* hybridation data we see low ARF activators levels in the central zone (described using $\pi_A \approx 0$), and much higher ones at the periphery (described using the reference value $\pi_A \approx 1$).
Results of simulations where this parameter is varied from 0 to 2 are displayed in Figures 3 and 4. It appears that for low values of π_A, an increase of auxin is barely perceived by the network. In particular, it appears in Figure 3 that almost no induction occurs when there is no ARF activator, and in Figure 4, fluctuations in auxin levels are strongly attenuated at low ARF activator levels.

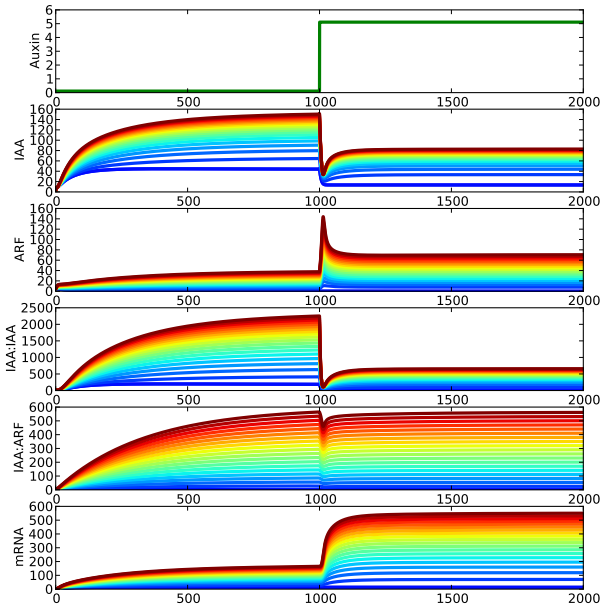

Figure 3: Time evolution of all variables of the model, under the influence of a step input of auxin level (first row). The parameter π_A is varied between 0 and 2 by steps of 0.1, using the colormap in Figure 2.

Note that in Figure 3 all variables are displayed. However for subsequent figures, only the levels of Aux/IAA and mRNA of target genes are shown, or even mRNA alone, since they represent the two crucial steps in the auxin perception process (i.e. more or less its input and output).

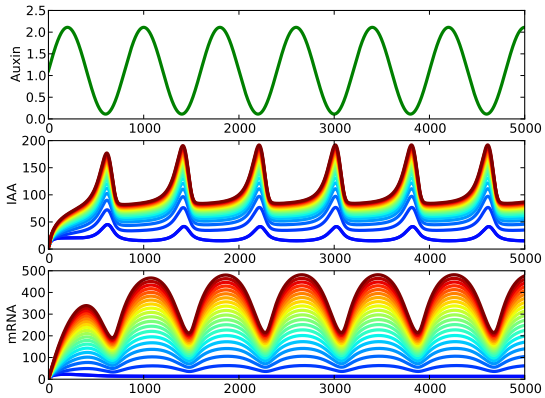

Figure 4: Time evolution of the variables I and R, under the influence of fluctuations of auxin level, represented using a sinus function (first row). π_A is varied between 0 and 2 by steps of 0.1, using the colormap in Figure 2.

Basal ARF repressors level κ_A^-

This parameter appears only in the transcription rate of the target gene, see (6). In this function, observe that other repressing terms, e.g. that associated to D_{IA}, are not direct concentrations, but are weighted by cooperativity coefficients and dissociation constants. Hence, the range of value over which κ_A^- was varied had to be chosen in accordance with this observation. To do so, we considered that ARF repressors and activators concentrations vary in the same range of values. Based on the values taken by the variable A in our simulations, we used $[0, 100]$ as a typical range, see Figure 3. Also, we used the parameters ω_A and B_d. Indeed, considering the repressing term associated to, say D_{IA}, in equation (6), and denoting A^- the concentration of ARF repressor, one gets the following analogy:

$$\kappa_A^- \equiv \frac{\omega_A A^-}{B_d}$$

The range $[0, 100]$ is plausible for ω_A, whereas B_d was fixed to 100 in (12), but lies plausibly within a $[10, 100]$ interval. Hence, varying κ_A^- in a range of $[0, 1000]$ is coherent with the rest of the present study.
The apparent effect of the basal level of ARF repressors expression, κ_A^- is to restrict the induction by auxin of its target gene, upon a step increase of auxin levels. Indeed, varying this parameter, one observes a decrease of the variable R, hence of the output of the signalling pathway. Observe in Figure 5 that the effect of auxin fluctuations is attenuated as κ_A^- increases; both the average level and amplitude of variations of the target gene mRNA are lowered by ARF repressors.

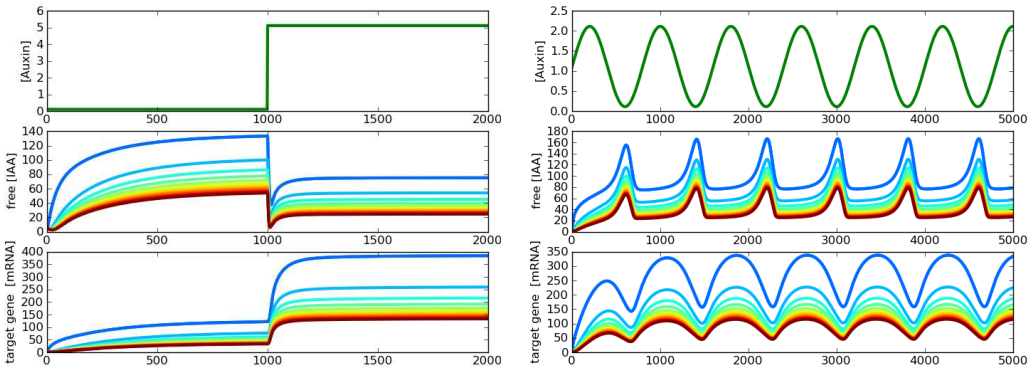

Figure 5: Time evolution of the variables I and R, under the influence of a input of auxin level (first row, on the left) and of periodic auxin fluctuations (first row, on the right). The parameter κ_A^- is varied between 0 and 1000 by steps of 100, using the colormap in Figure 2.

Aux/IAA decay rate δ_I

This parameter plays a dual role, influencing both the amplitude and the speed of the network response to auxin induction. In fact, high decay rates lead to a fast and sensible response of the system, whereas lowest decays almost have the effect of blocking the auxin signal, as seen in Figure 6. Noticeably, the Aux/IAA proteins are known to have varied half-lifes [2], and some have very specific expression patterns, e.g. IAA20 (whose half-life is higher than 12h [2]) or IAA30 (see Fig. 2 of the main paper). Hence, beyond the global features of auxin signaling underlined in the main text, the patterning of these proteins can lead to a local attenuation, or intensification, of auxin perception in the SAM. In other words, more specific responses can

occur in peculiar locations of the SAM, a fact that could be investigated more exhaustively in future works.

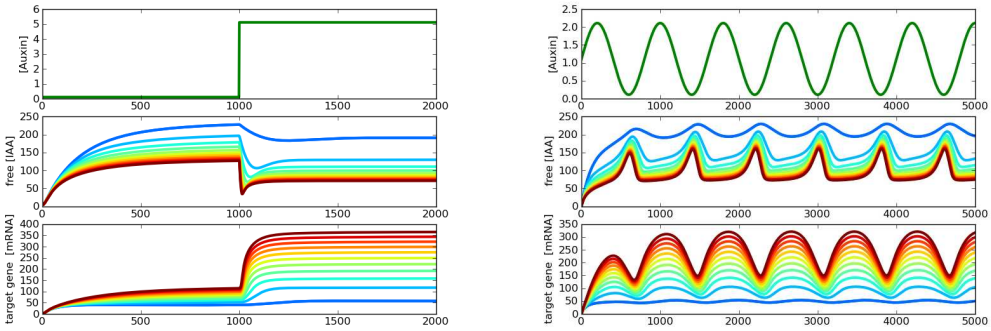

Figure 6: Time evolution of the variables I and R, under the influence of a input of auxin level (first row). The parameter δ_I is varied between 0.001 (i.e. half-life of $\approx$ 11h) and 0.051 (i.e. half-life of $\approx$ 13min) by steps of 0.005, using the colormap in Figure 2.

Other decay rates

The other decay rates of the system did not display as drastic an effect as the Aux/IAA half-lifes, although they tend to influence also the amplitude and speed of the response. However, this effect is very mild for δ_A and δ_{II}, see Figures 7(a) and 8(a) respectively, and more sensible for δ_R and δ_{IA}, see Figures 7(b) and 8(b) respectively. For these two parameters, the most noticeable effect is that for the lowest values, i.e. very stable mRNA or ARF:IAA dimer, the response seems quantitatively higher than for other plausible values.

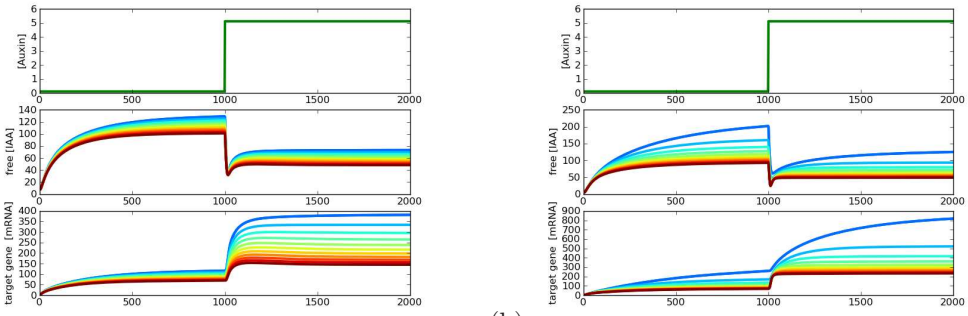

(a) (b)

Figure 7: Time evolution of the variables I and R, under the influence of a input of auxin level (first row). On the left the parameter δ_A is varied between 0.001 (i.e. half-life of $\approx$ 11h) and 0.051 (i.e. half-life of $\approx$ 13min) by steps of 0.005, using the colormap in Figure 2. On the right, δ_R is varied between 0.001 and 0.021 (i.e. half-life of $\approx$ 35min) by steps of 0.002, representing the range of Aux/IAA mRNA turnovers found in [4].

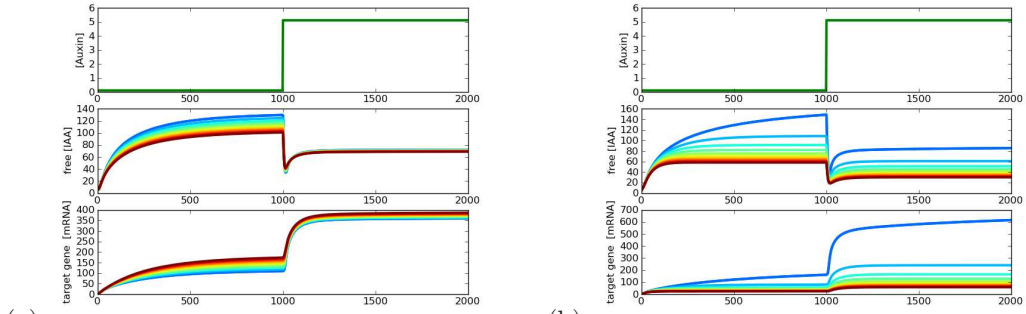

(a) (b)

Figure 8: Time evolution of the variables I and R, under the influence of a input of auxin level (first row). The parameters δ_{II} (on the left) and δ_{IA} (on the right) are varied between 0.001 (i.e. half-life of $\approx$ 11h) and 0.051 (i.e. half-life of $\approx$ 13min) by steps of 0.005, using the colormap in Figure 2.

Parameters for transcription factors efficiency

Let us now focus on the different parameters appearing in the transcription rate function $h(I, A, D_{IA})$, equation (6). These parameters, whose quantitative value has not been experimentally determined, do not seem to have an obvious qualitative influence on the system. Rather, they increase or decrease the transcription level in an intuitively expected way, as seen in Figures 9 and 10.

Transcription fold-changes f, f_A.

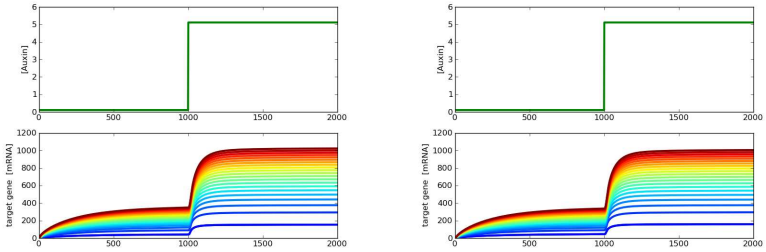

Figure 9: Time evolution of the sole variable R, under the influence of a input of auxin level (first row). The parameters f (on the left) and f_A (on the right) are varied between 1 and 101 by steps of 5, using the colormap in Figure 2.

Cooperativity coefficients $\omega_A, \omega_D, \omega_I$.

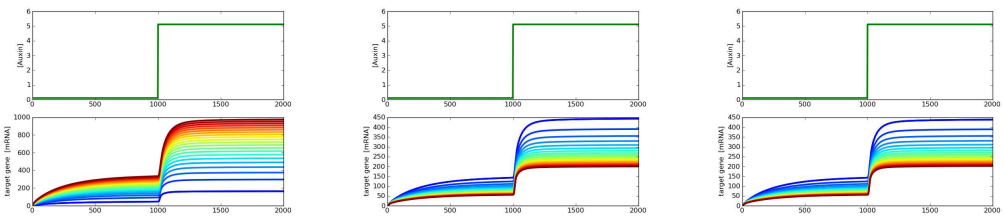

Figure 10: Time evolution of the sole variable R, under the influence of a input of auxin level (first row). The parameters ω_A, ω_I and ω_D (from left to right) are varied between 1 and 101 by steps of 5, using the colormap in Figure 2.

Dissociation constants K_{II}, K_{IA}

These constants are indicative of the stability of the ARF:IAA and IAA:IAA dimers; increasing these parameters amounts to consider less stable dimers, i.e. more reversible polymerization reactions. The quantitative value of the dissociation constants, although impacting quantitative levels of the different protein and dimer populations at steady state, do not alter qualitatively the dynamics of induction by auxin. Indeed, as seen in Figure 11, the shape of the response is barely altered by changing the dissociation constants, although this impact is most sensible for low values of the constants, i.e. when considering almost irreversible *versus* reversible dimer binding.
It is possible to give an interpretation of the peculiar role played by the extreme case when ARF:IAA or IAA:IAA dimers are almost irreversibly formed. Actually, in this case, the very stable dimers tend to form an overwhelming population, which supersedes other proteins in the medium. Then, in the case of IAA:IAA dimers, they form a buffer population which precludes repression by ARF:IAA dimers (explaining the higher level of transcription with low auxin). Since auxin induces a massive diminution of this population, the transcription levels are also largely increased. As for the ARF:IAA dimers, when very stable, they tend to occupy the promoter very stably, keeping transcription of the target genes very low.

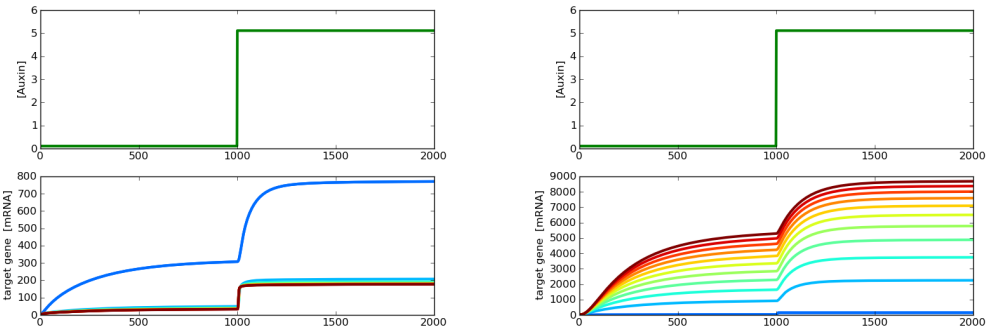

Figure 11: Time evolution of the variable R, under the influence of a input of auxin level (first row). The parameters K_{II} (left) and K_{IA} (right) are varied between 1 and 1001 by steps of 100, using the colormap in Figure 2.

Recapitulation on parameters

In brief, this study shows that the behaviour of the system is very robust, in the sense that it always responds to auxin variations in a similar way, by increasing the transcription level of target genes when auxin levels increase. It appears that most parameters of the system have a quantitative influence on this behaviour, impacting the amplitude and sometimes the time scale of the response. Considering our data sets, the basal levels of ARF activators, π_A, and ARF repressors, κ_A^- are particularly interesting parameters, since the central zone of the SAM can be approximated using low values of these two parameters, whereas the periphery corresponds to high values.

References

[1] N.E. Buchler, U. Gerland, T. Hwa, *Nonlinear protein degradation and the function of genetic circuits*, P.N.A.S, 102(27):9559-9564, 2005.

[2] K.A. Dreher, J. Brown, R.E. Saw, J. Callis, *The Arabidopsis Aux/IAA protein family has diversified in degradation and auxin responsiveness*, The Plant Cell, 18:699-714, 2006.

[3] A.M. Middleton, J. R. King, M.J. Bennett, M.R. Owen, *Mathematical Modelling of the Aux/IAA Negative Feedback Loop*, Bulletin of Mathematical Biology, published online (2010).

[4] R. Narsai, K.H. Howell, A.H.Millar, N. O'Toole, I. Small, J. Whelan, *Genome-wide analysis of mRNA decay rates and their determinants in Arabidopsis thaliana*, *The Plant Cell*, 19:3418-3436, 2007.

[5] J. Salmon, J. Ramos, J. Callis, *Degradation of the auxin response factor ARF1*, The Plant Journal, 54:118-128, 2008.

[6] T. Ulmasov, G. Hagen, T.J. Guilfoyle, *Dimerization and DNA binding of auxin response factors*, The Plant Journal, 19(3):309-319, 1999.